

Predictive Performance of Next Generation Physiologically Based Kinetic (PBK) Model Predictions in Rats Based on *In Vitro* and *In Silico* Input Data

Ans Punt ^{*,1}, Jochem Louisse,^{*} Nicole Pinckaers,^{*} Eric Fabian,[†] and Bennard van Ravenzwaay[†]

^{*}Wageningen Food Safety Research, Wageningen University and Research, 6700 AE Wageningen, the Netherlands, and [†]Experimental Toxicology and Ecology, BASF SE, 67056 Ludwigshafen, Germany

¹To whom correspondence should be addressed at Wageningen Food Safety Research, Wageningen University and Research, PO Box 230, 6700 AE Wageningen, the Netherlands. E-mail: ans.punt@wur.nl.

ABSTRACT

The goal of the present study was to assess the predictive performance of a minimal generic rat physiologically based kinetic (PBK) model based on *in vitro* and *in silico* input data to predict peak plasma concentrations (C_{\max}) upon single oral dosing. To this purpose, a dataset was generated of 3960 C_{\max} predictions for 44 compounds, applying different combinations of *in vitro* and *in silico* approaches for chemical parameterization, and comparison of the predictions to reported *in vivo* data. Best performance was obtained when (1) the hepatic clearance was parameterized based on *in vitro* measured intrinsic clearance values, (2) the method of Rodgers and Rowland for calculating partition coefficients, and (3) *in silico* calculated fraction unbound plasma and P_{app} values (the latter especially for very lipophilic compounds). Based on these input data, the median C_{\max} of 32 compounds could be predicted within 10-fold of the observed C_{\max} , with 22 out of these 32 compounds being predicted within 5-fold, and 8 compounds within 2-fold. Overestimations of more than 10-fold were observed for 12 compounds, whereas no underestimations of more than 10-fold occurred. Median C_{\max} predictions were frequently found to be within 10-fold of the observed C_{\max} when the scaled unbound hepatic intrinsic clearance ($Cl_{\text{int,u}}$) was either higher than 20 l/h or lower than 1 l/h. Similar findings were obtained with a test set of 5 in-house BASF compounds. Overall, this study provides relevant insights in the predictive performance of a minimal PBK model based on *in vitro* and *in silico* input data.

Key words: C_{\max} ; QIVIVE; rat; PBPK; PBK.

Substantial advances have been made over the last decades with the development of *in vitro* methods to capture biological effects of compounds that may serve as alternative test methods for animal toxicity testing (Jennings, 2015; Pamies *et al.*, 2018; Pamies and Hartung, 2017). However, the quantitative chemical distribution in the body is frequently ignored when interpreting *in vitro* effect data. Without these considerations, the *in vitro* biological effect data as stand-alone may lead to incorrect conclusions about the *in vivo* potencies of compounds,

because the ultimate *in vivo* effects will, besides the toxicodynamic effects (in the target tissue), also depend on the toxicokinetics (ie, the concentration of the chemical at the site of action) (Bessemers *et al.*, 2014; Blaauboer, 2010; Yoon *et al.*, 2015). Applying physiologically based kinetic (PBK) modeling concomitantly to *in vitro* toxicity testing provides an effective framework for the extrapolation of *in vitro* biological effect concentrations to equivalent (oral) doses (eg, DeJongh *et al.*, 1999; Fabian *et al.*, 2019; Forsby and Blaauboer, 2007; Gubbels-van Hal *et al.*, 2005;

© The Author(s) 2021. Published by Oxford University Press on behalf of the Society of Toxicology.

This is an Open Access article distributed under the terms of the Creative Commons Attribution-NonCommercial License (<https://creativecommons.org/licenses/by-nc/4.0/>), which permits non-commercial re-use, distribution, and reproduction in any medium, provided the original work is properly cited. For commercial re-use, please contact journals.permissions@oup.com

Louisse et al., 2010; Punt et al., 2019; Verwei et al., 2006; Wetmore et al., 2015). By simulating the plasma (or tissue) concentrations at different doses, one can infer the doses that are needed to reach the *in vitro* effect concentrations in the plasma (or tissue) and whether these effect doses are expected to be reached at defined exposure estimates.

Although PBK modeling is increasingly acknowledged to play a crucial role in the transition toward animal-free testing strategies for chemical safety evaluations to perform the required quantitative *in vitro* to *in vivo* extrapolations (QIVIVE), the development of PBK models solely on the basis of *in vitro* and/or *in silico* input data remains a challenge (Paini et al., 2019; Peters and Dolgos, 2019). Initial estimates of plasma and tissue concentrations of compounds can effectively be made with minimal generic PBK models that are defined based on (1) a first-order intestinal absorption rate (k_a) and a fraction absorbed (f_a), (2) intrinsic hepatic clearance (Cl_{int}), (3) tissue: plasma partition coefficients, (4) the fraction unbound plasma (f_{up}), and (5) passive renal excretion (defined as the glomerular filtration rate times the unbound concentration of the compound in plasma [$GFR \times c_{plasma} \times f_{up}$]). For each of these different kinetic processes, different input approaches can be applied. For example, k_a and f_a can be estimated from Caco-2 absorption studies or calculated based on *in silico* tools (Hou et al., 2004). Cl_{int} data can either be obtained with primary hepatocytes, S9, or microsomes, or can be predicted using *in silico* methods (Zhang et al., 2018). The f_{up} can also be calculated *in silico* or experimentally derived using, for example, microdialysis experiments (Rotroff et al., 2010). Partition coefficients are generally calculated *in silico*, for which different approaches exist (Berezhkovskiy, 2004; Poulin and Theil, 2002; Rodgers and Rowland, 2006; Schmitt, 2008). It must be noted that available *in silico* tools are often trained based on available *in vitro* data, indicating that the *in vitro* and *in silico* methods cannot be regarded as being totally independent.

Uncertainties exist with respect to the impact of these different approaches on the model predictions, the quality of the input data as well as the difficulty of determining whether additional kinetic processes need to be added to the model (eg, extrahepatic metabolism and/or transporter-mediated kinetics). As a result, PBK model predictions still need to be evaluated on a case-by-case basis against *in vivo* data (eg, plasma concentrations) (Peters and Dolgos, 2019; Tsamandouras et al., 2015). Moreover, when certain kinetic processes cannot be parameterized based on *in vitro* or *in silico* experiments, they are usually obtained by fitting model predictions to *in vivo* data (Peters and Dolgos, 2019; Tsamandouras et al., 2015). To facilitate the transition toward nonanimal testing strategies, it is important to move away from this case-by-case evaluation and optimization of PBK models against *in vivo* data, and to identify other strategies for the evaluation of the adequacy of *in vitro*- and *in silico*-based PBK models to estimate *in vivo* kinetics.

The goal of the present study was to assess the general predictive performance of a minimal generic rat PBK model based on *in vitro* and *in silico* input data to predict peak plasma concentrations (C_{max}) upon single dosing. To this end, C_{max} predictions in rats upon single oral dosing were made for a set of 44 model compounds based on a range of input approaches for estimating the chemical specific parameters (Cl_{int} , f_{up} , partition coefficients, and k_a) and compared with observed C_{max} values reported in the literature for these compounds in rats. We characterized the contribution of different input approaches to the wide variation in C_{max} predictions for individual compounds. In addition, we assessed whether we could find a relation between

chemical (kinetic) characteristics (such as extent of metabolic clearance, charge, lipophilicity, or uptake rate of the compounds) and the chance that the C_{max} is predicted within 10-fold or not. The results obtained were applied on 5 in-house BASF compounds as case study.

MATERIALS AND METHODS

Chemical dataset. A dataset of 44 model compounds was formed based on the availability of *in vivo* data (maximum plasma concentrations [C_{max}]) in rats after single oral dosing, allowing to evaluate the performance of the C_{max} predictions by the PBK model based on different *in vitro* and/or *in silico* input approaches. The majority of compounds in the dataset (38 compounds) were selected based on available plasma C_{max} data for rat in the database of the R `httk` package by Pearce et al. (2017). The dataset was extended with 4 food-relevant compounds (bisphenol A, genistein, daidzein, and ochratoxin A), for which *in vivo* oral kinetic studies in rats were available in the literature. In addition, rosuvastatin and fluvastatin were included for which transporter-mediated processes in liver and kidney play a main role in the kinetics (Chan et al., 2019). The final list of model compounds and related *in vivo* C_{max} data (and related oral doses) is available as [Supplementary Material](#). In addition to the 44 model compounds, 5 in-house BASF compounds were included as case study to test the minimal PBK modeling approach.

Generic PBK model code and input parameters. PBK model predictions in rat were performed based on a published generic (human) PBK model code by Jones and Rowland-Yeo (2013) that was implemented in R (R Core Team, 2021, version 4.1.1) and converted from human to rat by Punt et al. (2021) by inclusion of rat-specific parameters as obtained from Musther et al. (2017). The model consists of 13 compartments, corresponding to the major organs in the body and an arterial and venous blood compartment. The model requires chemical-specific parameters for intestinal uptake, distribution (ie, partition coefficients, blood-plasma ratio [assumed to be 1 in the present study for all compounds], f_{up}), hepatic clearance, and renal clearance (assumed to be the glomerular filtration rate times the free plasma concentration). [Table 1](#) provides an overview on how these different input parameters were parameterized using a range of *in vitro* and/or *in silico* methods. Further details on these input approaches are given in the text below. The differential equations of the model are solved with the `deSolve` package (Soetaert et al., 2010). The R code of the PBK model is provided in the Github repository (https://github.com/wfsrqivive/rat_PBK.git; last accessed December 22, 2021).

Absorption from the gastrointestinal tract was described in the model by a first-order uptake process from the intestine to the liver compartment and requires an absorption rate constant (k_a) and fraction absorbed (f_a) as input (Jones and Rowland-Yeo, 2013). For the parameterization of these input constants an *in silico* approach based on a QSAR from Hou et al. (2004) was applied that predicts the Caco-2 apparent permeability (P_{app}) based on the topological polar surface area (TPSA) of the compounds ([equation 1](#)). Both ADMET Predictor software (v.9.0, Simulations Plus, Lancaster, California; www.simulations-plus.com; last accessed December 22, 2021) and ChemAxon (ChemAxon Ltd., Budapest, Hungary; www.chemaxon.com; last accessed December 22, 2021) were used to generate these TPSA values. Given that both software packages yielded the same TPSA results, no further distinctions were made

Table 1. Input Approaches Applied in the PBK Model Predictions

Applied Input	Method Reference	Method Name Used in the Figures	Number of Compounds for Which the Respective Data Are Available
Intestinal uptake (k_a and f_a)			
QSAR based on the topological surface area (TPSA)	Hou et al. (2004)	QSAR	44
Caco-2 P_{app}	This work	<i>In vitro</i>	26
Physicochemical characteristics			
log P, log D, pK_a , TPSA	ADMET predictor	ADMET	44
log P, log D, pK_a , TPSA	ChemAxon	ChemAxon	44
Tissue: plasma partition coefficients			
Berezhkovskiy	Berezhkovskiy (2004)	Berezhkovskiy	44
Rodgers and Rowland	Rodgers and Rowland (2006)	RodgersRowland	44
Schmitt	Schmitt (2008)	Schmitt	44
Intrinsic hepatic clearance (Cl_{int})			
(Cryopreserved) primary hepatocytes	Data derived from the htk package (Pearce et al., 2017)	Hep	38
Liver S9	This work	S9	25
<i>In silico</i> predicted CYP clearance	ADMET predictor	<i>In silico</i>	44
Fraction unbound plasma			
<i>In vitro</i> with rapid equilibrium dialysis	Data derived from the htk package (Pearce et al., 2017)	<i>In vitro</i>	39
<i>In silico</i> predicted based on log P, log D, and pK_a	Lobell and Sivarajah (2003)	<i>In silico</i>	44

between these 2 sets of results for assessing the PBK model's predictive capacity. For 26 out of the 44 compounds, the QSAR-based approach was compared with *in vitro* measured apparent permeability (P_{app}) coefficients in Caco-2 transwell absorption experiments. Details on Caco-2 experiments are provided as [Supplementary Material](#). Both the QSAR-derived P_{app} values and the *in vitro* measured values were scaled to an uptake rate constant (k_a) and fraction absorbed (f_a) based on equations 2–5.

$$\log P_{app} \text{ (cm/s)} = -4.36 - 0.01 * \text{TPSA} \quad (1)$$

$$\log P_{eff, human} (10^{-4} \text{ cm/s}) = 0.4926 * \log P_{app} (10^{-6} \text{ cm/s}) - 0.1454 \quad (2)$$

$$P_{eff, rat} = P_{eff, human} / 11.04 \quad (3)$$

$$k_a \text{ (/h)} = P_{eff} * 2 \text{ (cm/s)} / R \text{ (cm)} * 3600 \text{ (s/h)} \quad (4)$$

$$f_a = 1 - \left(1 + (2 * P_{eff} * (T_{si})) / (7 * R) \right)^{-7}, \quad (5)$$

in which [equation 1](#) is derived from [Hou et al. \(2004\)](#), [equation 2](#) scales the Caco-2 apparent permeability (QSAR predicted or *in vitro* measured) to the human effective permeability based on [Sun et al. \(2002\)](#), [equation 3](#) scales the human effective permeability to a rat effective permeability based on equation that is derived from [Wahajuddin et al. \(2011\)](#), and [equations 4 and 5](#) describe how the effective permeabilities are converted to k_a and f_a as derived from [Yu and Amidon \(1999\)](#). For the calculation of the k_a and f_a values with [equations 4 and 5](#), an intestinal radius (R) of 0.18 cm for rat was used and a small intestinal transit time (T_{si}) of 1.47 h ([Grandoni et al., 2019](#)).

Physicochemical data (log P, log D, and pK_a values, TPSA), which are used as input to calculate the f_u and tissue: plasma partition coefficients and intestinal uptake were derived with ADMET Predictor software (v9.0, Simulation Plus, Lancaster,

California; [www.simulations-plus.com](#); last accessed December 22, 2021) and with ChemAxon (ChemAxon Ltd., Budapest, Hungary; [www.chemaxon.com](#); last accessed December 22, 2021). Given that slight differences occur between the results of these 2 software packages with respect to the log P and pK_a and resulting log D estimates, the influence of these differences on the PBK model predictions was evaluated. The log P, log D, and pK_a (s) that were obtained for the 44 compounds with each of the 2 software packages are provided in the Github repository ([https://github.com/wfsrqvive/rat_PBK.git](#); last accessed December 22, 2021).

An *in silico* approach for calculating the f_u values was compared with measured values. For the *in silico* calculations of f_u , a method of [Lobell and Sivarajah \(2003\)](#) was used. Log P and information on the pK_a (s) are required input parameters for this calculation. The codes can be found in the Github repository ([https://github.com/wfsrqvive/rat_PBK.git](#); last accessed December 22, 2021). The *in vitro*-derived rat-specific f_u values for 39 compounds were taken from the htk package with the original data measured by [Wetmore et al. \(2013\)](#), [Wood et al. \(2017\)](#), and [Honda et al. \(2019\)](#).

For the calculation of partition coefficients, 3 approaches were compared including the *in silico* approaches of (1) [Rodgers and Rowland \(2006\)](#), (2) [Berezhkovskiy \(2004\)](#), which corresponds to the corrected method of [Poulin and Theil \(2002\)](#), and (3) the *in silico* approach of [Schmitt \(2008\)](#). Log P and information on the pK_a (s) are required input approaches for these calculations. The R codes for these different calculation methods were obtained from [Utsey et al. \(2020\)](#) and were adjusted to fit the pipeline of the PBK model calculations of the current study. The codes can be found in the Github repository as part of the input parameters ([https://github.com/wfsrqvive/rat_PBK.git](#); last accessed December 22, 2021). As input for the prediction of the partition coefficients, the standardized tissue composition data from [Utsey et al. \(2020\)](#) were used. In case of the method of

Schmitt, the membrane affinity (log MA) was calculated from the log P based on a QSAR from Yun and Edginton (2013) as provided in the R code.

Three different approaches to obtain model parameter values for hepatic intrinsic clearance were compared. These include (1) an *in silico* approach, (2) an *in vitro* approach based on clearance studies with primary rat hepatocytes, and (3) an *in vitro* approach based on clearance studies with rat liver S9. *In silico* clearance calculations (rat microsomal P450 clearance) were carried out with the ADMET Predictor (v.9.0, Simulations Plus, Lancaster, California). The primary rat hepatocyte clearance data were derived from the database of the R htkk package, containing the values that were originally measured by Wetmore et al. (2013), Wood et al. (2017), and Honda et al. (2019). For 25 compounds out of the 44 compounds, the intrinsic hepatic clearance was measured in the current study in incubations with rat liver S9 in the presence of a mix of cofactors (NADPH, UDPGA, and PAPS) as described in the Supplementary Material. The *in vitro* compounds for which the S9 clearance rates were determined, were selected based on the expected clearance to include compounds with low (0–20 $\mu\text{l}/\text{min}/\text{mg}$ S9 protein), medium (20–100 $\mu\text{l}/\text{min}/\text{mg}$ S9 protein), and high (>100 $\mu\text{l}/\text{min}/\text{mg}$ S9 protein) *in vitro* intrinsic hepatic clearance. All *in vitro*-derived hepatic clearance values were corrected for unspecific binding to hepatocytes or S9 using a calculation method of Kilford et al. (2008) for primary hepatocytes and a method of Halifax and Houston (2006) for the S9 clearance measurements. Although the latter calculation method was developed to predict the unbound intrinsic clearance in microsomal incubations, it was assumed to also be applicable to S9 incubations. The codes can be found in the Github repository as part of the input parameters (https://github.com/wfsrqvive/rat_PBK.git; last accessed December 22, 2021). The *in silico* calculated clearance rates already represent the unbound clearance rates and no correction was required.

Rat PBK model predictions and data analysis. By combining different input approaches, a total of 3960 C_{max} predictions were made for the different model compounds at the same exposure conditions as used the *in vivo* studies from which the reported C_{max} values were obtained. For each chemical, the predicted C_{max} was divided by the observed C_{max} as marker of the quality of the of PBK model prediction for that compound. As a result of the different input combinations a range in predicted:observed ratios is obtained for each chemical of which the median was calculated. When these median predicted C_{max} outcomes were within 5-fold of the observed C_{max} , the PBK model predictions were considered adequate for a first estimation of internal dose metrics by a minimal generic PBK model. C_{max} predictions within 10-fold of the observed C_{max} are less precise, but still considered relevant. A 2-fold cut-off value is also included in the different figures of the present study, as this cut-off value is frequently used in a regulatory context, though particularly for PBK models that are optimized to available *in vivo* data (Shebley et al., 2018). Median predicted C_{max} values that are more than 10-fold higher than the observed C_{max} values were considered as overestimated, and median C_{max} values that are more than 10-fold lower than the observed C_{max} values were considered as underestimated, though the latter did not occur in the present data set (see Results section). The effect of different input approaches on the C_{max} predictions was determined, by comparing for each input approach and compound the median C_{max} and predicted:observed ratios and determining the differences between the input approaches in predicted median C_{max} values.

A sensitivity analysis was performed for the predictions by changing the input value of a parameter by 1% and determining the relative change in C_{max} , expressed as the normalized sensitivity coefficient (NSC). The sensitivity analysis was performed at an equal oral dose of 1 mg/kg bw for all compounds and input combinations. Each parameter was analyzed individually, keeping the other parameters to their initial values. The R codes for the above analyses can be found in the in the Github repository (https://github.com/wfsrqvive/rat_PBK.git; last accessed December 22, 2021).

RESULTS

Performance of the Generic PBK Model Based on Different Input Approaches

By combining different input approaches to parameterize the PBK model (Table 1), a total of 3960 C_{max} predictions were made for 78 *in vivo* C_{max} results (ie, exposure situations described in the literature with reported C_{max} values) for a total of 44 compounds. In Figure 1, the ratios between PBK model-predicted C_{max} values and *in vivo*-observed C_{max} values are shown. The results for bisphenol A, curcumin, daidzein, fluvastatin, genistein, resveratrol, rosuvastatin, and ochratoxin A represent the comparison of the predicted C_{max} with observed C_{max} values from multiple *in vivo* studies, whereas for the other compounds *in vivo* data were obtained from single studies. Figure 1 reveals a large variation (1–6 orders of magnitude) in the prediction:observed ratios. The largest range in predicted:observed ratios are observed for bisphenol A, curcumin, permethrin, and resmethrin. For these compounds, some of the individual C_{max} predictions were 210-, 33436-, 553-, and 806-fold higher than the observed C_{max} , respectively, and some predictions were 76-, 1.8-, 1183-, and 208-fold lower, respectively. Within the dataset as a whole, median C_{max} predictions of 30 compounds were within 10-fold, whereas 14 compounds were predominantly overestimated, that is, having a median predicted C_{max} that is >10-fold higher than the observed C_{max} . Twenty-three compounds could be predicted within 5-fold and 12 compounds within 2-fold of the observed C_{max} .

Sensitivity Analysis

A sensitivity analysis was performed by changing the input value of a parameter by 1% and determining the relative change in C_{max} , expressed as the NSC. Figure 2A shows the results for the most influential input parameters that affect the C_{max} predictions (maximum observed NSCs >0.5 in absolute value). The NSCs of remaining input parameters are presented in Supplementary Figure 1. The results of the sensitivity analysis show that the chemical-specific input parameters related to the extent of metabolic clearance are most influential. This includes the intrinsic clearance parameter (Cl_{int}) itself, but also parameters that relate to the free available concentration for the metabolic conversion (f_{up} , K_{pli}) and parameters that determine the blood flow and the volume of the liver (FQh, QC). Other important input parameters that affect the C_{max} predictions relate the oral absorption (k_a and f_a). B:P ratio also showed to be a sensitive parameter. This parameter was set to a default value of 1 for all compounds in the present study, because measured data on B:P ratios are generally lacking and no *in silico* tools are available to estimate the B:P ratio. The observed differences between compounds in sensitivity toward the input parameters (see range in NSCs in Figure 2A) were found to primary relate to the intrinsic metabolic clearance of each compound (Figure 2B).

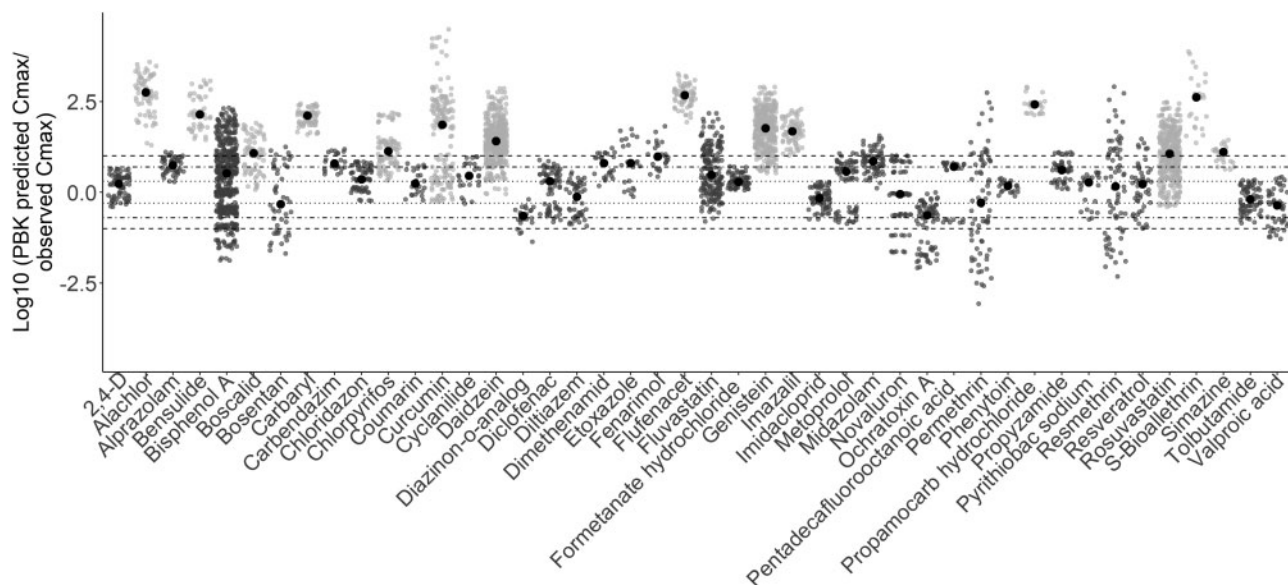


Figure 1. Ratios between PBK model-predicted C_{max} values and *in vivo*-observed C_{max} values observed for 44 reference compounds in rat. Per chemical, different predicted C_{max} values are obtained by running simulations with the different input approaches (*in vitro* or *in silico* approaches to parameterize a certain input parameter) as presented in Table 1. Each predicted C_{max} is then compared with the *in vivo* C_{max} values for the chemical in the dataset. The median of these predicted/observed ratios is depicted along the individual datapoints. Datapoints within the dotted, dot-dashed, or dashed horizontal lines are within 2-fold, 5-fold or 10-fold of the observed C_{max} , respectively. Compounds for which the median predicted C_{max} is more than 10-fold overestimated are depicted in light gray.

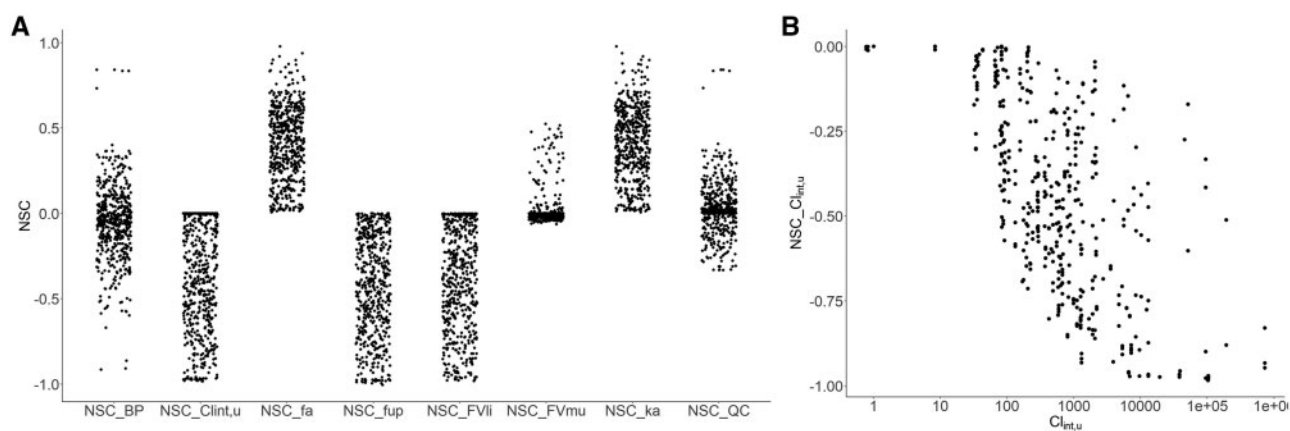


Figure 2. A, Normalized sensitivity coefficients (NSCs) of the C_{max} predictions to different input parameters for the different compounds. B, NSCs for $Cl_{int,u}$ plotted against $Cl_{int,u}$ values used as input. The datapoints in the figures correspond to the NSCs for a random selection of 12 C_{max} simulations based on different input approaches per chemical. Abbreviations: BP, blood:plasma ratio; $Cl_{int,u}$, scaled unbound intrinsic liver; f_a , fraction absorbed; f_{up} , fraction unbound plasma; FV_{ii} , volume fraction liver; FV_{mu} , volume fraction muscle; k_a , intestinal uptake rate; QC, cardiac output.

The sensitivity increases with increasing $Cl_{int,u}$ until a maximum sensitivity is reached for compounds with a high $Cl_{int,u}$ (Figure 2B). A similar relation is observed between the $Cl_{int,u}$ of the compounds and the sensitivity toward the other input parameters that are depicted in Figure 2A, with low clearance compounds being less sensitive to changes in the input parameters than high clearance compounds (Supplementary Figure 2).

Effect of the Input Approaches on the C_{max} Predictions

Given the wide range in C_{max} outcomes and corresponding predicted:observed ratios in Figure 1 and given the sensitivity of the C_{max} predictions to chemical-specific input parameters like $Cl_{int,u}$, f_{up} , f_a , and k_a , it is important to identify how the C_{max} predictions are affected by the different input approaches. To this end, we defined for each input approach the range in C_{max} predictions that are obtained and evaluated if systematic differences occurred between

the different input approaches that were used to parameterize the generic PBK model. Figure 3 highlights those predictions for which differences (>3-fold) in predicted:observed ratios are observed for a specific chemical as a result of the applied input approach. These results reveal that differences in C_{max} predictions (and corresponding predicted:observed ratios) most frequently occur as a result of differences in calculation methods for the partition coefficients (Figure 3A) and the methods used to parameterize hepatic clearance (Figure 3B).

In case of the different approaches for the calculation of partition coefficients, the method of Rodgers and Rowland performed best. The median C_{max} of 32 compounds was predicted within 10-fold of the observed C_{max} values with the Rodgers and Rowland method. With the methods of Berezhkovskiy and Schmitt, 30 and 27 compounds were predicted within 10-fold of the observed C_{max} , respectively. Particularly for acidic

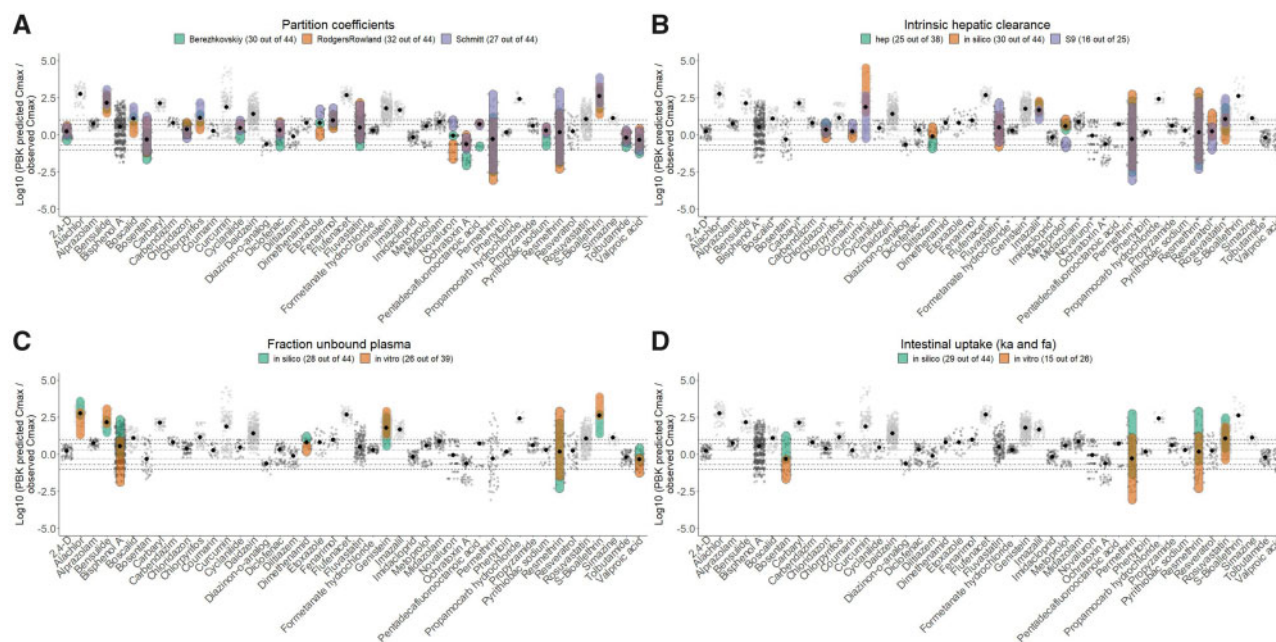


Figure 3. Differences in predicted:observed C_{max} ratios related to the applied input approaches for A) partition coefficients, B) intrinsic hepatic clearance, C) fraction unbound in plasma, and D) intestinal uptake. Highlighted are those results for which more than a 3-fold difference in mean C_{max} predictions was observed between the applied input approaches. In case of (B), S9-derived intrinsic clearance data are included in the comparison of input approaches for the compounds that are marked with an asterisk. The different input approaches are provided in the legends, including, between brackets, the number of compounds for which the C_{max} was predicted within 10-fold of the observed C_{max} .

compounds ($pK_a < 6$), like ochratoxin A and pentadecafluorooctanoic acid, low C_{max} predictions are obtained with the method of Berezhkovskiy compared with the other input approaches. For the highly lipophilic compounds ($\log P > 5$), like etoxalone, novaluron, permethrin, and resmethrin, the method of Schmitt appears to result in overpredictions of the C_{max} .

In case of the parameterization of the intrinsic hepatic clearance, the C_{max} predictions based on *in silico*-derived hepatic intrinsic clearance values appear to be frequently different from the predictions based on *in vitro* S9 and/or hepatocyte intrinsic clearance data. Particularly in case of curcumin, metoprolol, and resveratrol, the *in silico*-calculated clearance values lead to an overprediction of the *in vivo*-observed C_{max} . In case of curcumin, this overprediction is even up to 33436-fold. For the compounds for which both *in vitro* S9 and hepatocyte data are available, significant differences in intrinsic hepatic clearance were only found for metoprolol (Figure 3B).

Occasional outliers were found to occur in the C_{max} predictions as a result of the uptake parameters (k_a and f_a) (Figure 3B), and the f_{up} (Figure 3C). The most important outlier was found for bisphenol A, for which the C_{max} was significantly (up to 806-fold) underestimated when the *in vitro*-measured f_{up} is used in the simulations compared with the *in silico*-calculated f_{up} . Given that the relatively high *in vitro*-measured f_{up} of 0.71 does not match with another reported *in vitro* f_{up} by Csanády et al. (2002) of 0.05 and the *in silico*-predicted f_{up} of 0.04, the simulations based on the f_{up} of 0.71 were considered to be incorrect. In case of permethrin and resmethrin, the *in silico*-predicted uptake rates (Figure 3B) were found to provide C_{max} results that are closest to the *in vivo*-observed C_{max} values. A key challenge with these compounds, that might have caused the high variation in C_{max} predictions, is the relatively high lipophilicity of these compounds ($\log P$ values larger than 5), which may hamper

reliable performance of the *in vitro* studies with Caco-2 cells, providing unreliable P_{app} values to derive the uptake rate.

Performance of the Optimized PBK Model

Figure 4 depicts the results of the dataset in which the most significant outliers as described above are removed. This includes a removal of the simulations based on (1) the methods of Berezhkovskiy and Schmitt for the partition coefficients, (2) the *in silico*-derived intrinsic hepatic clearance data, and (3) *in vitro*-measured f_{up} values. In addition, the *in vitro*-derived uptake rates for permethrin and resmethrin were removed as identified significant outliers. The results of the reduced dataset that was obtained shows a significant reduction in the variation in C_{max} predictions and the related predicted:observed C_{max} ratios. The remaining relatively high variation in predicted:observed C_{max} ratios as observed for bisphenol A, daidzein, genistein, and resveratrol in Figure 4 can be attributed to the variation in the related *in vivo* studies.

The median C_{max} prediction for curcumin, boscalid, and chlorpyrifos improved and could be predicted within 10-fold in the optimized dataset. In contrast, the median C_{max} of fluvastatin becomes more than 10-fold overestimated in the reduced dataset. Overall, the removal of the most significant outliers mainly resulted in an increased number of predictions within 10-fold. Median C_{max} predictions of 32 compounds were within 10-fold within the reduced dataset, whereas 12 compounds were predominantly overestimated, that is, having a median predicted C_{max} that is >10-fold higher than the observed C_{max} . Twenty-two compounds could be predicted within 5-fold and 8 compounds within 2-fold of the observed C_{max} .

We assessed whether we could find a relation between chemical (kinetic) characteristics (such as extent of metabolic clearance, charge, lipophilicity, or uptake rate of the compounds) and the chance of being predicted within 10-fold as

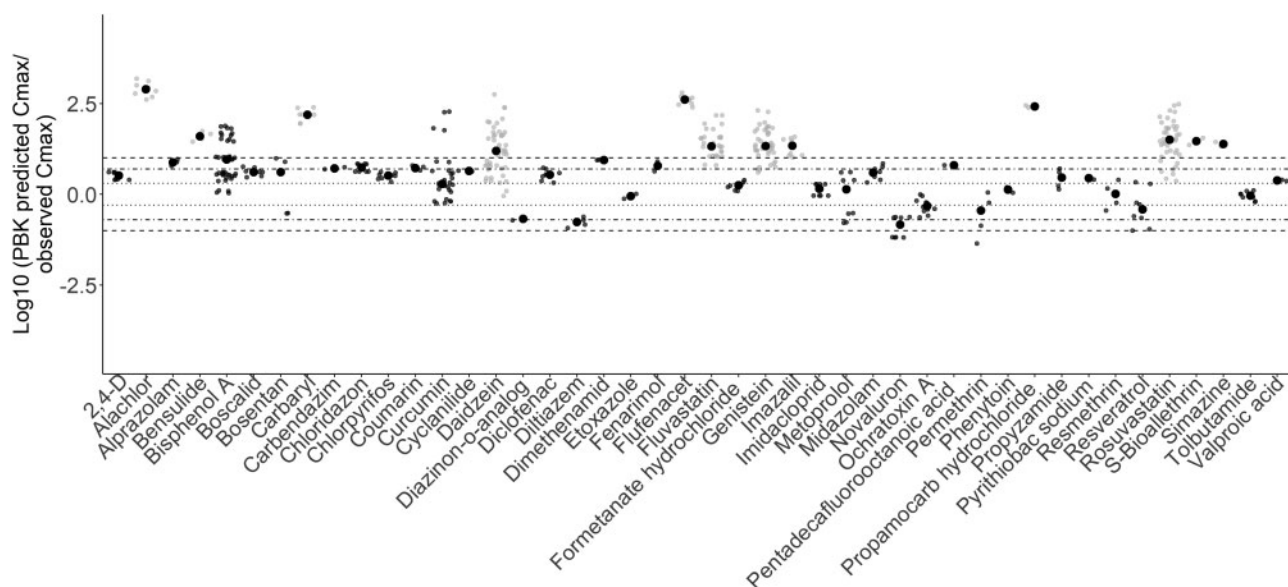


Figure 4. Ratios between PBK model-predicted C_{\max} values and *in vivo*-observed C_{\max} values observed for 44 reference compounds in rat after removal of the simulations based on input methods that led to significant worst predictions as described in the main text.

cut-off value within which most of the compounds could be predicted. Comparison of the clearance rates with the predicted:observed ratios of the compounds revealed that the C_{\max} of 9 out of the 10 compounds with the highest clearance values ($Cl_{\text{int,u}} > 201/\text{h}$) are predicted within 10-fold. In addition, the C_{\max} of 15 out of the 19 compounds with a $Cl_{\text{int,u}} < 1/\text{h}$ are predicted within 10-fold. Together, these low and high clearance groups represent 63% of the compounds that were predicted within 10-fold (Supplementary Material). For the compounds that had a clearance between 1 and 20 l/h, no relations were identified between chemical characteristics (clearance, charge lipophilicity, etc.) and the chance of being predicted within 10-fold (Supplementary Material).

Application of the Minimal PBK Model Approach on In-House BASF Compounds as Case Study

The minimal PBK model approach was applied on 5 in-house BASF compounds as case study to test whether similar results are obtained with respect to the range in predicted:observed ratios and the type of compounds that are likely to be predicted within 10-fold (ie, low or high clearance compounds). Table 2 provides an overview of the *in vitro* and *in silico* input data that are available for the 5 compounds as well as the C_{\max} predictions that are obtained with the generic PBK model. The physicochemical characteristics were estimated with ChemAxon, the intrinsic hepatic metabolic clearance data were derived from experiments with rat liver S9, and Caco-2 apparent permeability coefficients were derived from *in vitro* experiments (BASF1-3 and 5) or estimated *in silico* (BASF4). The partition coefficients were calculated with the calculation method of Rodgers and Rowland. Based on the analysis with the 44 reference compounds, these applied input approaches can be considered to provide the best predictions when applied in this minimal PBK model.

Based on the scaled unbound hepatic clearance values (Table 2), it was expected that the C_{\max} predicted for BASF1, 3, and 4 had a high chance to be predicted within 10-fold compared with the *in vivo* data as these are all low clearance compounds ($Cl_{\text{int,u}} < 1/\text{h}$) (see Performance of the Optimized PBK

Model section). Running the PBK models indicated that the C_{\max} of these 3 compounds are indeed within 10-fold of the observed C_{\max} . The scaled $Cl_{\text{int,u}}$ values of BASF2 and BASF5 of 2.7 and 14.1 l/h were in the range of scaled $Cl_{\text{int,u}}$ values of compounds for which it was more difficult to discriminate whether overprediction is likely to occur or not (see Performance of the Optimized PBK Model). BASF2 was overpredicted (18- to 65-fold, depending on the dose), whereas the C_{\max} of BASF5 was predicted within 5-fold of the observed C_{\max} . Additional information (eg, on the solubility, transporter involvement, or extrahepatic metabolism) is expected to be essential to further discriminate whether certain compounds are likely to be predicted by the generic PBK model within 10-fold of the observed C_{\max} or not.

DISCUSSION

Predictions of internal dosimetry, such as C_{\max} , are crucial in the transition toward next generation (animal-free) testing strategies for chemical safety evaluations to convert *in vitro* toxicity data into *in vivo* dose-response or at least potency information (eg, DeJongh et al., 1999; Fabian et al., 2019; Forsby and Blaauboer, 2007; Gubbels-van Hal et al., 2005; Louise et al., 2010; Punt et al., 2019; Verwei et al., 2006; Wetmore et al., 2015). At present, PBK model predictions still need to be evaluated on a case-by-case basis against *in vivo* kinetic data (Peters and Dolgos, 2019; Tsamandouras et al., 2015). For a transition to next generation (animal-free) regulatory risk evaluations to happen, other means to gain confidence in PBK model predictions are needed. The goal of the present study was to assess the predictive performance of a minimal generic rat PBK model based on *in vitro* and *in silico* input data to predict peak plasma concentrations (C_{\max}) upon single oral dosing.

Different cut-off values (2-, 5-, and 10-fold) were used as performance indicators in the current study. Discussions are presently still ongoing on what level of deviation between predicted and observed kinetics is acceptable within a regulatory context (Shebley et al., 2018). The required precision of PBK model predictions may depend on the use application. The 10-fold cut-off

Table 2. Chemical-Specific Data of 5 In-House BASF Compounds and Information on PBK Model-Predicted C_{\max} Values and Comparison With *In Vivo* C_{\max} Values

PBK Model Input Parameters	Test Compounds				
	BASF1	BASF2	BASF3	BASF4	BASF5
Log P ChemAxon	1.19	2.96	3.45	-2.82	3.99
pK_a (s) ChemAxon	3.38 (A)	10.7 (A); -0.11 (B)	Neutral	Contains N^+	0.44 (B)
<i>In vitro</i> Caco-2 P_{app} (10^{-6} cm/s)	46.8	37.9	25	43 ^a	13.8
k_a (/h) and f_a scaled based on the Caco-2 P_{app}	1.72 and 0.91	1.55 and 0.88	1.27 and 0.84	1.65 and 0.90	0.94 and 0.75
f_u (in silico predicted)	0.124	0.124	0.079	0.982	0.047
Liver S9 clearance (μ l/min/S9 mg protein)	1.9	17.3	0	0	53.9
Scaled unbound hepatic clearance ($Cl_{int,u}$, l/h)	0.2	2.3	0	0	14.1
Doses (mg/kg bw)	4; 40; 200	50; 500	3; 30; 300	1.2; 12	5; 50
C_{\max} Predicted (mg/l)	12; 119; 594	7; 72	0.4; 3.7; 37	0.9; 9.4	0.2; 1.6
C_{\max} Observed (mg/l)	7; 14; 260	0.4; 1.1	0.2; 3.6; 26.0	0.23; 2.3	0.09; 0.4
Predicted:observed ratio	1.7; 8.5; 2.3	18; 65	2; 1; 1.4	4; 4	2; 4

A, acid; B, base.

^a*In silico* estimated based on a topological surface area of 0 (zero) \AA^2 , using the calculation method of Hou et al. (2004).

value used in the present study provides a relevant indication of whether compounds can be captured with the minimal generic PBK model. For the compounds falling outside this value, deviations between the predicted and observed C_{\max} values ranged between 16-fold (daidzein) and 783-fold (alachlor), which cannot be resolved by optimization of the different input parameters. A 2-fold cut-off value is frequently requested within a regulatory context to demonstrate that the proposed model is fit for purpose (Peters and Dolgos, 2019). A key challenge with this 2-fold is that the differences between *in vivo* studies, to which the model predictions are compared, tend to be higher than 2-fold themselves, possibly related to differences in biology or technical aspects (Shebley et al., 2018). For example, in the present study, the ranges in predicted:observed ratios for bisphenol A (between 0.15- and 12-fold) were primarily caused by the 60-fold difference in the respective *in vivo* results, to which the predictions were compared with (Domoradzki, 2004; Pottenger, 2000; Sun Dong Yoo et al., 2001; Tominaga et al., 2006; Upmeier et al., 2000). Taking the different cut-off values into account, the results reveal that most of the compounds fall within the 10-fold range, whereas predictions within the 5- or 2-fold are more difficult to obtain. Although some level of uncertainty in PBK model predictions can be considered acceptable for situations where the margin of exposure between exposure and biological effects is large (Wetmore et al. 2015), further work will be needed to determine how the generic PBK model can be further improved to increase the number of predictions that can be made within 5- or 2-fold to increase the overall precision of the model. Furthermore, based on the chosen cut-off value(s) of required model precision, related uncertainty factors may need to be applied when using *in vitro*- and *in silico*-based PBK model results in a regulatory context.

A key challenge with respect to PBK model development is to determine the design of the model structure for a specific compound. The results of the present study revealed that the minimal generic PBK model, based on partition coefficients, Cl_{int} , F_u , and P_{app} as main chemical-specific input, worked best for compounds that are either extensively metabolized ($Cl_{int,u} > 20$ l/h) or compounds that are metabolized to a limited extent ($Cl_{int,u} < 1$ l/h), as these compounds were frequently found to be predicted within a 10-fold range. Three out of the 5 in-house BASF compounds fell into this category of low-clearance compounds and were also predicted within 10-fold of the observed

C_{\max} (BASF1, BASF3, and BASF4). In case of the chemicals that are 10-fold overpredicted it is expected that, for example, a lack of inclusion of extrahepatic metabolism and/or transporter-mediated processes in the PBK model are underlying causes of the deviations between predicted and observed C_{\max} values. In addition, transporter-mediated processes might also be relevant to be included for some of the low-clearance compounds, which have been reported to be substrates of transporter proteins (like pentadecafluorooctanoic acid, ochratoxin A, and tolbutamide) (Anzai et al., 2010; Bi et al., 2018; Worley and Fisher, 2015). Although the C_{\max} of many of these compounds could be predicted within 10-fold, refinement of the kinetic predictions is expected to be achieved by also including these transporter-mediated processes, particularly to better simulate repeated exposures. Further work will be needed to explore whether recommendations can be made based on these characteristics on the design of a PBK model for a specific compound, particularly to determine when a minimal PBK model will be sufficient and when additional kinetic processes need to be considered.

Comparison of the different input approaches revealed a high influence of the selected input parameters on the PBK model predictions. For example, the results of the present study show that the method of Berezhkovskiy should not be used for acids ($pK_a < 6$) as this might lead to underprediction of the C_{\max} . This is probably caused by the fact that the impact of drug ionization on partitioning is not explicitly taken into account in the method of Berezhkovskiy (Utsey et al., 2020). The calculation method of Schmitt was found to frequently lead to relative overpredictions of the C_{\max} of highly lipophilic compounds ($\log P > 5$) and may therefore not be appropriate for this group of compounds. The results of the calculation method of Schmitt largely depend on the membrane affinity as input. As this value was not available for all compounds, it was calculated in the present study based on $\log P$ based on a QSAR from Yun and Edginton (2013). Highly lipophilic compounds might not fall into the applicability domain of this QSAR. In case of the hepatic clearance, the *in vitro*-observed data are preferred above *in silico*-generated clearance data. The C_{\max} values of various compounds were overpredicted as a result of the use of *in silico* clearance values, and more importantly a direct comparison of the *in silico*-estimated clearance values with the *in vitro* values revealed a relatively poor correlation ($R^2 = 0.3$, Supplementary Figure 3), indicating that challenges still exist with the

predictive value of *in silico* tools for Cl_{int} . In case of the Fu_p and P_{app} values, a significant influence of *in vitro* experimental variation on the model predictions was observed. Particularly, for highly lipophilic compounds, like permethrin and resmethrin, the *in vitro* input data led to underpredictions by the PBK model. These results indicate the importance of standardizing and harmonizing the *in vitro* approaches to obtain robust results, including *in vitro* protocol adjustments to work with very lipophilic compounds (Ferguson et al., 2019; Wambaugh et al., 2019).

Overall, the current study provided relevant insights into the predictive performance of a minimal PBK model and the influence of different input approaches on the model predictions. Best performance was obtained when the hepatic clearance was parameterized based on (1) *in vitro* (hepatocytes or liver S9)-measured intrinsic clearance values, (2) the method of Rodgers and Rowland for calculating partition coefficients, and (3) *in silico*-calculated fraction unbound plasma and P_{app} values (the latter especially for very lipophilic compounds). Further work will particularly be needed to find ways to determine, in the absence of prior knowledge on the chemical's *in vivo* toxicokinetics, when and which additional kinetic processes (like extrahepatic metabolism or transporter-mediated processes) need to be added to obtain adequate predictions of the *in vivo* kinetics.

SUPPLEMENTARY DATA

Supplementary data are available at Toxicological Sciences online.

DECLARATION OF CONFLICTING INTERESTS

The authors declared no potential conflicts of interest with respect to the research, authorship, and/or publication of this article.

FUNDING

Dutch Ministry of Agriculture, Nature and Food Quality (Topsector Agri&Food Project No. AF-18070).

REFERENCES

- Anzai, N., Jutabha, P., and Endou, H. (2010). Molecular mechanism of ochratoxin A transport in the kidney. *Toxins* 2, 1381–1398.
- Berezhkovskiy, L. M. (2004). Volume of distribution at steady state for a linear pharmacokinetic system with peripheral elimination. *J. Pharm. Sci.* 93, 1628–1640.
- Bessems, J. G., Loizou, G., Krishnan, K., Clewell, H. J., Bernasconi, C., Bois, F., Coecke, S., Collnot, E. M., Diembeck, W., Farcial, L. R., et al. (2014). PBTK modelling platforms and parameter estimation tools to enable animal-free risk assessment. Recommendations from a joint EPAA - EURL ECVAM ADME workshop. *Regul. Toxicol. Pharmacol.* 68, 119–139.
- Bi, Y. A., Mathialagan, S., Tylaska, L., Fu, M., Keefer, J., Vildhede, A., Costales, C., Rodrigues, A. D., and Varma, M. V. S. (2018). Organic anion transporter 2 mediates hepatic uptake of tolbutamide, a CYP2C9 probe drug. *J. Pharmacol. Exp. Ther.* 364, 390–398.
- Blaauboer, B. J. (2010). Biokinetic modeling and *in vitro-in vivo* extrapolations. *J. Toxicol. Environ. Heal. Part B Crit. Rev.* 13, 242–252.
- Chan, J. C. Y., Tan, S. P. F., Upton, Z., and Chan, E. C. Y. (2019). Bottom-up physiologically-based biokinetic modelling as an alternative to animal testing. *ALTEX* 36, 597–612.
- Csanády, G., Oberste-Frielinghaus, H., Semder, B., Baur, C., Schneider, K., and Filser, J. (2002). Distribution and unspecific protein binding of the xenoestrogens bisphenol A and daidzein. *Arch. Toxicol.* 76, 299–305.
- DeJongh, J., Nordin-Andersson, M., Ploeger, B. A., and Forsby, A. (1999). Estimation of systemic toxicity of acrylamide by integration of *in vitro* toxicity data with kinetic simulations. *Toxicol. Appl. Pharmacol.* 158, 261–268.
- Domoradzki, J. Y., Thornton, C. M., Pottenger, L. H., Hansen, S. C., Card, T. L., Markham, D. A., Dryzga, M. D., Shiotsuka, R. N., and Waechter, J. M. (2004). Age and dose dependency of the pharmacokinetics and metabolism of bisphenol A in neonatal Sprague-Dawley rats following oral administration. *Toxicol. Sci.* 77, 230–242.
- Fabian, E., Gomes, C., Birk, B., Williford, T., Hernandez, T. R., Haase, C., Zbrank, R., van Ravenzwaay, B., and Landsiedel, R. (2019). *In vitro-to-in vivo* extrapolation (IVIVE) by PBTK modeling for animal-free risk assessment approaches of potential endocrine-disrupting compounds. *Arch. Toxicol.* 93, 401–416.
- Ferguson, K. C., Luo, Y.-S., Rusyn, I., and Chiu, W. A. (2019). Comparative analysis of Rapid Equilibrium Dialysis (RED) and solid phase micro-extraction (SPME) methods for *In Vitro-In Vivo* extrapolation of environmental chemicals. *Toxicol. In Vitro.* 60, 245–251.
- Forsby, A., and Blaauboer, B. (2007). Integration of *in vitro* neurotoxicity data with biokinetic modelling for the estimation of *in vivo* neurotoxicity. *Hum. Exp. Toxicol.* 26, 333–338.
- Grandoni, S., Cesari, N., Brogin, G., Puccini, P., and Magni, P. (2019). Building in-house PBPK modelling tools for oral drug administration from literature information. *Admet DMPK* 7, 4–21.
- Gubbels-van Hal, W., Blaauboer, B. J., Barentsen, H. M., Hoitink, M. A., Meerts, I., and van der Hoeven, J. (2005). An alternative approach for the safety evaluation of new and existing chemicals, an exercise in integrated testing. *Regul. Toxicol. Pharmacol.* 42, 284–295.
- Hallifax, D., and Houston, J. B. (2006). Binding of drugs to hepatic microsomes: Comment and assessment of current prediction methodology with recommendation for improvement. *Drug Metab. Dispos.* 34, 724–726.
- Honda, G. S., Pearce, R. G., Pham, L. L., Setzer, R. W., Wetmore, B. A., Sipes, N. S., Gilbert, J., Franz, B., Thomas, R. S., and Wambaugh, J. F. (2019). Using the concordance of *in vitro* and *in vivo* data to evaluate extrapolation assumptions. *PLoS One* 14, e0217564.
- Hou, T. J., Zhang, W., Xia, K., Qiao, X. B., and Xu, X. J. (2004). ADME evaluation in drug discovery. 5. Correlation of caco-2 permeation with simple molecular properties. *J. Chem. Inf. Comput. Sci.* 44, 1585–1600.
- Jennings, P. (2015). The future of *in vitro* toxicology. *Toxicol. In Vitro* 29, 1217–1221.
- Jones, H., and Rowland-Yeo, K. (2013). Basic concepts in physiologically based pharmacokinetic modeling in drug discovery and development. *CPT Pharmacometrics Syst. Pharmacol.* 2, e63.
- Kilford, P. J., Gertz, M., Houston, J. B., and Galetin, A. (2008). Hepatocellular binding of drugs: Correction for unbound fraction in hepatocyte incubations using microsomal binding or drug lipophilicity data. *Drug Metab. Dispos.* 36, 1194–1197.

- Lobell, M., and Sivarajah, V. (2003). In silico prediction of aqueous solubility, human plasma protein binding and volume of distribution of compounds from calculated pKa and AlogP98 values. *Mol. Divers.* **7**, 69–87.
- Louise, J., de Jong, E., van de Sandt, J. J. M., Blaauboer, B. J., Woutersen, R. A., Piersma, A. H., Rietjens, I. M. C. M., and Verwei, M. (2010). The use of in vitro toxicity data and physiologically based kinetic modeling to predict dose-response curves for in vivo developmental toxicity of glycol ethers in rat and man. *Toxicol. Sci.* **118**, 470–484.
- Musther, H., Harwood, M. D., Yang, J., Turner, D. B., Rostami-Hodjegan, A., and Jamei, M. (2017). The constraints, construction, and verification of a strain-specific physiologically based pharmacokinetic rat model. *J. Pharm. Sci.* **106**, 2826–2838.
- Paini, A., Leonard, J. A., Joossens, E., Bessems, J. G. M., Desalegn, A., Dorne, J. L., Gosling, J. P., Heringa, M. B., Klaric, M., Kliment, T., et al. (2019). Next generation physiologically based kinetic (NG-PBK) models in support of regulatory decision making. *Comput. Toxicol.* **9**, 61–72.
- Pamies, D., Bal-Price, A., Chesné, C., Coecke, S., Dinnyes, A., Eskes, C., Grillari, R., Gstraunthaler, G., Hartung, T., Jennings, P., et al. (2018). Advanced good cell culture practice for human primary, stem cell-derived and organoid models as well as microphysiological systems. *ALTEX* **35**, 353–378.
- Pamies, D., and Hartung, T. (2017). 21st century cell culture for 21st century toxicology. *Chem. Res. Toxicol.* **30**, 43–52.
- Pearce, R. G., Setzer, R. W., Strobe, C. L., Sipes, N. S., and Wambaugh, J. F. (2017). Httk: R package for high-throughput toxicokinetics. *J. Stat. Softw.* **79**, 1–26.
- Peters, S. A., and Dolgos, H. (2019). Requirements to establishing confidence in physiologically based pharmacokinetic (PBPK) models and overcoming some of the challenges to meeting them. *Clin. Pharmacokinet.* **58**, 1355–1371.
- Pottenger, L. H., Domoradzki, J. Y., Markham, D. A., Hansen, S. C., Cagen, S. Z., and Waechter, J. M. (2000). The relative bioavailability and metabolism of bisphenol A in rats is dependent upon the route of administration. *Toxicol. Sci.* **54**, 3–18.
- Poulin, P., and Theil, F.-P. (2002). Prediction of pharmacokinetics prior to in vivo studies. II. Generic physiologically based pharmacokinetic models of drug disposition. *J. Pharm. Sci.* **91**, 1358–1370.
- Punt, A., Aartse, A., Bovee, T. F. H., Gerssen, A., van Leeuwen, S. P. J., Hoogenboom, R. L. A. P., and Peijnenburg, A. A. C. M. (2019). Quantitative in vitro-to-in vivo extrapolation (QIVIVE) of estrogenic and anti-androgenic potencies of BPA and BADGE analogues. *Arch. Toxicol.* **93**, 1941–1953.
- Punt, A., Pinckaers, N., Peijnenburg, A., and Lousse, J. (2021). Development of a web-based toolbox to support quantitative in-vitro-to-in-vivo extrapolations (QIVIVE) within nonanimal testing strategies. *Chem. Res. Toxicol.* **34**, 460–472.
- R Core Team. (2021). R: A language and environment for statistical computing. R Foundation for Statistical Computing, Vienna, Austria. Available at: <https://www.R-project.org/>. Accessed December 22, 2021.
- Rodgers, T., and Rowland, M. (2006). Physiologically based pharmacokinetic modelling 2: Predicting the tissue distribution of acids, very weak bases, neutrals and zwitterions. *J. Pharm. Sci.* **95**, 1238–1257.
- Rotroff, D. M., Wetmore, B. A., Dix, D. J., Ferguson, S. S., Clewell, H. J., Houck, K. A., Lecluyse, E. L., Andersen, M. E., Judson, R. S., Smith, C. M., et al. (2010). Incorporating human dosimetry and exposure into high-throughput in vitro toxicity screening. *Toxicol. Sci.* **117**, 348–358.
- Schmitt, W. (2008). General approach for the calculation of tissue to plasma partition coefficients. *Toxicol. In Vitro* **22**, 457–467.
- Shebley, M., Sandhu, P., Emami Riedmaier, A., Jamei, M., Narayanan, R., Patel, A., Peters, S. A., Reddy, V. P., Zheng, M., de Zwart, L., et al. (2018). Physiologically based pharmacokinetic model qualification and reporting procedures for regulatory submissions: A consortium perspective. *Clin. Pharmacol. Ther.* **104**, 88–110.
- Soetaert, K., Petzoldt, T., and Setzer, R. W. (2010). Solving differential equations in R: Package deSolve. *J. Stat. Softw.* **33**, 1–25.
- Sun, D., Lennernas, H., Welage, L. S., Barnett, J. L., Landowski, C. P., Foster, D., Fleisher, D., Lee, K.-D., and Amidon, G. L. (2002). Comparison of human duodenum and Caco-2 gene expression profiles for 12,000 gene sequences tags and correlation with permeability of 26 drugs. *Pharm. Res.* **19**, 1400–1416.
- Tominaga, T., Negishi, T., Hirooka, H., Miyachi, A., Inoue, A., Hayasaka, I., and Yoshikawa, Y. (2006). Toxicokinetics of bisphenol A in rats, monkeys and chimpanzees by the LC-MS/MS method. *Toxicology* **226**, 208–217.
- Tsamandouras, N., Rostami-Hodjegan, A., and Aarons, L. (2015). Combining the ‘bottom up’ and ‘top down’ approaches in pharmacokinetic modelling: Fitting PBPK models to observed clinical data. *Br. J. Clin. Pharmacol.* **79**, 48–55.
- Upmeier, A., Degen, G. H., Diel, P., Michna, H., and Bolt, H. M. (2000). Toxicokinetics of bisphenol A in female DA/Han rats after a single i.v. and oral administration. *Arch. Toxicol.* **74**, 431–436.
- Utsey, K., Gastonguay, M. S., Russell, S., Freling, R., Riggs, M. M., and Elmokadem, A. (2020). Quantification of the impact of partition coefficient prediction methods on physiologically based pharmacokinetic model output using a standardized tissue composition. *Drug Metab. Dispos.* **48**, 903–916.
- Verwei, M., van Burgsteden, J. A., Krul, C. A., van de Sandt, J. J., and Freidig, A. P. (2006). Prediction of in vivo embryotoxic effect levels with a combination of in vitro studies and PBPK modelling. *Toxicol. Lett.* **165**, 79–87.
- Wambaugh, J. F., Wetmore, B. A., Ring, C. L., Nicolas, C. I., Pearce, R. G., Honda, G. S., Dinallo, R., Angus, D., Gilbert, J., Sierra, T., et al. (2019). Assessing Toxicokinetic Uncertainty and Variability in Risk Prioritization. *Toxicol. Sci.* **172**, 235–251.
- Wahajuddin, Singh, S. P., Patel, K., Pradhan, T., Siddiqui, H. H., and Singh, S. K. (2011). Prediction of human absorption of a trioxane antimalarial drug (CDRI 99/411) using an in-house validated in situ single-pass intestinal perfusion model. *Arzneimittelforschung* **61**, 532–537.
- Wetmore, B. A., Wambaugh, J. F., Allen, B., Ferguson, S. S., Sochaski, M. A., Setzer, R. W., Houck, K. A., Strobe, C. L., Cantwell, K., Judson, R. S., et al. (2015). Incorporating high-throughput exposure predictions with dosimetry-adjusted in vitro bioactivity to inform chemical toxicity testing. *Toxicol. Sci.* **148**, 121–136.
- Wetmore, B. A., Wambaugh, J. F., Ferguson, S. S., Li, L., Clewell, H. J., Judson, R. S., Freeman, K., Bao, W., Sochaski, M. A., Chu, T. M., et al. (2013). Relative impact of incorporating pharmacokinetics on predicting in vivo hazard and mode of action from high-throughput in vitro toxicity assays. *Toxicol. Sci.* **132**, 327–346.
- Wood, F. L., Houston, J. B., and Hallifax, D. (2017). Clearance prediction methodology needs fundamental improvement: Trends common to rat and human hepatocytes/microsomes and implications for experimental methodology. *Drug Metab. Dispos.* **45**, 1178–1188.
- Worley, R. R., and Fisher, J. (2015). Application of physiologically-based pharmacokinetic modeling to explore

- the role of kidney transporters in renal reabsorption of perfluorooctanoic acid in the rat. *Toxicol. Appl. Pharmacol.* **289**, 428–441.
- Yoo, S. D., Shin, B. S., Lee, B. M., Lee, K. C., Han, S. Y., Kim, H. S., Kwack, S. J., and Park, K. L. (2001). Bioavailability and mammary excretion of bisphenol A in Sprague-Dawley rats. *J. Toxicol. Environ. Health A* **64**, 417–426.
- Yoon, M., Blaauboer, B. J., and Clewell, H. J. (2015). Quantitative in vitro to in vivo extrapolation (QIVIVE): An essential element for in vitro-based risk assessment. *Toxicology* **332**, 1–3.
- Yu, L. X., and Amidon, G. L. (1999). A compartmental absorption and transit model for estimating oral drug absorption. *Int. J. Pharm.* **186**, 119–125.
- Yun, Y. E., and Edginton, A. N. (2013). Correlation-based prediction of tissue-to-plasma partition coefficients using readily available input parameters. *Xenobiotica* **43**, 839–852.
- Zhang, F., Bartels, M., Clark, A., Erskine, T., Auernhammer, T., Bhatarai, B., Wilson, D., and Marty, S. (2018). Performance evaluation of the GastroPlus™ software tool for prediction of the toxicokinetic parameters of chemicals. *SAR QSAR Environ. Res.* **29**, 875–893.